

# Long-range properties and data validity for hydrogeological time series: the case of the Paglia river

Marcel Ausloos\*

*University of Leicester, School of Business  
Leicester, LE11 7RH, United Kingdom*

Email: [ma683@le.ac.uk](mailto:ma683@le.ac.uk)

*Group of Researchers for Applications of Physics in Economy and Sociology (GRAPES),  
rue de la Belle Jardiniere 483, B-4031 Angleur, Belgium*

Email: [marcel.ausloos@ulg.ac.be](mailto:marcel.ausloos@ulg.ac.be)

Roy Cerqueti

*University of Macerata, Department of Economics and Law, Macerata, I-62100.*

Email: [roy.cerqueti@unimc.it](mailto:roy.cerqueti@unimc.it)

Claudio Lupi

*University of Molise, Department of Economics, Campobasso, I-86100.*

Email: [lupi@unimol.it](mailto:lupi@unimol.it)

November 29, 2016

## Abstract

This paper explores a large collection of about 377,000 observations, spanning more than 20 years with a frequency of 30 minutes, of the streamflow of the Paglia river, in central Italy. We analyze the long-term persistence properties of the series by computing the Hurst exponent, not only in its original form but also under an evolutionary point of view by analyzing the Hurst exponents over a rolling windows basis. The methodological tool adopted for the persistence is

---

\*Corresponding author

the detrended fluctuation analysis (DFA), which is classically known as suitable for our purpose. As an ancillary exploration, we implement a control on the data validity by assessing if the data exhibit the regularity stated by Benford's law. Results are interesting under different viewpoints. First, we show that the Paglia river streamflow exhibits periodicities which broadly suggest the existence of some common behavior with El Niño and the North Atlantic Oscillations: this specifically points to a (not necessarily direct) effect of these oceanic phenomena on the hydrogeological equilibria of very far geographical zones: however, such an hypothesis needs further analyses to be validated. Second, the series of streamflows shows an antipersistent behavior. Third, data are not consistent with Benford's law: this suggests that the measurement criteria should be opportunely revised. Fourth, the streamflow distribution is well approximated by a discrete generalized Beta distribution: this is well in accordance with the measured streamflows being the outcome of a complex system.

**Keywords:** River streamflow, Hurst exponent, Benford's law, Detrended fluctuation analysis, Discrete generalized Beta distribution.

## 1 Introduction

Hydrogeological paths exhibit often a complex behavior. Such irregularities are driven by the presence of several factors of uncertainty in the climate dynamics. River streamflows represent paradigmatic examples of this evidence. In fact, human activities and natural events drive the fluctuations, sometimes with catastrophic effects, of such phenomena.

This paper elaborates some crucial observations from these premises. In particular, we develop an analysis of the streamflow of the Paglia river, a major tributary of Tiber, whose watercourse is entirely localized in Central Italy. Data are the official measurements of the streamflow of the river at Ponte dell'Adunata, near Orvieto, a historical town in Umbria region. The time interval covered by the measurements is January 1st, 1992 (12:00am) – May 13, 2014 (h11:30pm), and the periodicity of the observations is 30 minutes. However, the pervasive presence of missing values in the first part of the series prevented us from using the data prior to November 2, 1992 (h12:30pm).

We specifically focus on the so-called *long run dependence property* of the series, which gives a thoughtful view of the behavior of the autocorrelation function. Such a statistical property can be suitably employed for making

forecasts on the future evolution of the streamflow. The perspective presented here is in line with the original, path-breaking study by [[1]], who explored the long-run dependence of the runoffs of the Nile river. The analysis is based on the assessment of the value of the constant  $H \in (0, 1)$  — the so-called *Hurst exponent* — which represents the rate of decay of the autocorrelation function of the series as a function of the time-lag. If  $H > 1/2$ , the series is said to present a persistent behavior, which basically means that the history of the past will “statistically” repeat in the future;  $H < 1/2$  stands for antipersistence, the opposite of persistence;  $H = 1/2$  is the pure random case.

Since its inception, several contributions dealing with the assessment of the Hurst exponent in a number of very different contexts have appeared in the literature; a complete list is too long to be mentioned here.

In detecting long-run dependence, river discharges are of particular interest. In fact, they offer very specific time series with peculiar features. First of all, they have periodicities, with different periods. Such a property is due to the strong relationship between the river streamflow dynamics, the weather and the precipitation, but also to the effects of the global warming over the hydrogeological systems of the planet Earth [[1]-[7]].

Under the point of view of the human activities, it is self-evident how the fluctuations of the streamflow of any river affect (positively or negatively) the socio-economic system of the surrounding areas. In this respect, the Paglia river and the municipality of Orvieto represent very interesting cases to treat. In fact, there is a high level of hydrogeological risk related to Paglia’s floods in the Orvieto area: the last important flood took place on November 12, 2012, causing injuries and huge damages to the local economy. An effective plan to deal with this recurring phenomenon should necessarily move from a deep knowledge of the dynamics of the river and a forecast of when and how a flood will take place in the future.

From a purely technical viewpoint, we proceed by applying the *Detrended Fluctuation Analysis* (DFA) — introduced by [[8]] — which is classically acknowledged to be a powerful tool for the estimation of the Hurst exponent, whence long term persistence effects, mainly in the presence of non-stationarities. The appeal of the DFA lies in its conceptualization. Indeed, the underlying theoretical framework can be found in the theory of random walks [[9, 10]]. In such a context, time series are opportunely aggregated. This reduces the noise level due to biases in measurements.

In the context of DFA applications, it is worth mentioning [[11]-[14]].

As an ancillary analysis, we also consider the “validity” of the data measured at Ponte dell’Adunata. We do not infirm its interest, of course, but we wish to point some possible defects impairing a finer analysis as that pre-

sented here. In fact, the subsequent discussion and conclusions might be the first of this sort in the present context. For this purpose, and in accordance with [[15]] observations of river streamflows in the USA, we check if data fit Benford’s law [[16]].

In fact, such an empirical rule (on the logarithmic distribution of the first digit in lengthy data) has been found to hold in a wide spectrum of cases; see, e.g., (and the references therein) [[17]-[24]]. When violated, the presence of some sort of data manipulation or mistakes in data collection has to be debated.

The rest of the paper is organized as follows: in the next Section (Sect. 2) we introduce the dataset and the methodologies. In Section 3 we present and discuss the results. In the last Section (Sect. 4), we offer some concluding remarks.

## 2 Data and methodologies

The Paglia river is an important right-side tributary of Tiber, the third longest river in Italy. It is about 86km-long, with many tributaries along its course. It is characterized by a very variable streamflow (see Table 1 and Figure 1) which gives Paglia a crucial role in determining the floods of Tiber. Data, obtained from an hydrometer station run by the Umbria regional authority, measure the streamflow (expressed in  $m^3/s$ ) of the Paglia river at Ponte dell’Adunata, just downstream of the confluence of Chiani river, a 42km-long left-side tributary of Paglia.

Because of the presence of many long measurement interruptions during the first ten months of 1992, in our analysis we consider measurements recorded at each half hour starting on November 2, 1992 (h12:30pm), until May 13, 2014 (h11:30pm). There are still a few missing values in the selected period (in 7 occurrences the interruption of the measurements lasted for more than 2 days). Such missing values have been linearly interpolated on the series expressed in logarithms.<sup>1</sup> The resulting series (plotted in logs in Figure 1) includes 377,399 observations.

Data have been analyzed under several perspectives: first, we carry out a graphical analysis of the main features of the streamflows.

Then, we estimate the spectrum of the daily averages, in order to assess the presence of seasonal and non-seasonal periodicities.

---

<sup>1</sup>All computations have been carried out using R ver. 3.3.1 [[25]] and packages **benford.analysis** [ [26]], **fractal** [[27]], **ggplot2** [[28]], **imputeTS** [[29]], **moments** [[30]], **psd** [[31]], **xts** [[32]].

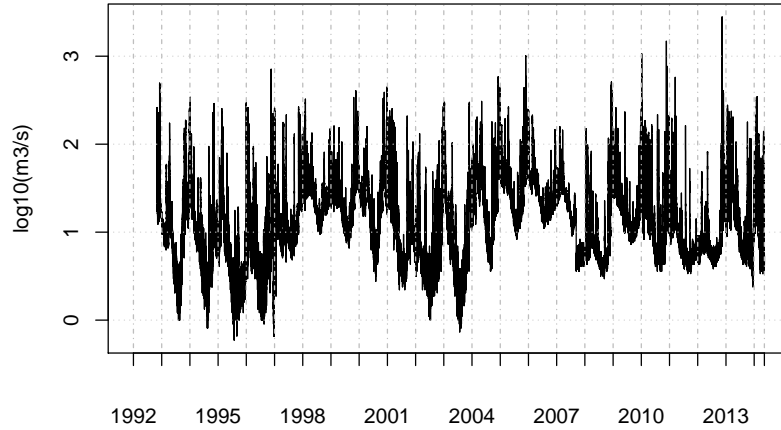


Figure 1: Streamflow (expressed in  $\log_{10}(m^3/s)$ ) of the Paglia river measured at every half hour between November 2, 1992 and May 13, 2014. Ticks on the x-axis identify the beginning of the years, except the the last tick that indicates the last available observation.

Min.	1st Q.	Median	Mean	3rd Q.	Max.
0.59	6.29	12.31	20.53	23.93	2794.00
$\sigma$	Skewness	Kurtosis	Date of Max.	Date of Min.	Data points
34.63	20.81	989.48	2012/11/12	1995/07/28	377399

Table 1: Main descriptive statistics of the Paglia river streamflow ( $m^3/s$ ) as measured at Ponte dell'Adunata, near Orvieto (November 2, 1992 – May 13, 2014).

For what concerns the estimation of the Hurst exponent, we perform a detrended fluctuation analysis (DFA) over 90-day long rolling windows. At each iteration the window is moved forward by a 1-day step. For a more intuitive visualization, when needed, windows will be numbered according to a chronological criterion. Specifically, we start from window 1 — the one at the beginning of the sample period. Then, we shift the window by one day and add 1 to the windows counter at any shift. According to this mechanism, window 1 is the one spanning days 1–90, window 2 spans days 2–91, window 3 insists on days 3–92, and so on. The Hurst exponent,  $H$ , is estimated in each window, resulting in a series of 7,773 estimated values of the Hurst exponent. In order to check the sensitivity of the results on the window length, we repeat the same analysis using 180 and 400-day long windows.

We also carry out a check for “data validity”. For this purpose, we adopt the point of view of [[15]], who suggest that streamflow statistics of US rivers are broadly consistent with Benford’s law. For this reason we check if the data gathered for the Paglia river are also consistent with Benford’s law. This part of the analysis is carried out on the observed data only, without any imputation of missing values. In particular we carry out a first-two digits test, which is more informative than the combination of both the first digit and the second digit tests; see e.g., especially Chapter 4 in [[33]].

Finally, we check if the observed data approximately follow a discrete generalized Beta distribution (DGBD), typical of the output of complex systems [[34]].

### 3 Results and discussion

The streamflow series expressed in logarithms shows several features of the Paglia river fluctuations (see Figure 1). However, more information can be gathered by looking at the basic monthly statistics of the data: it is evident that the series exhibits some periodicity, visually two regimes: a stationary one, representing the “normal” streamflow of the Paglia river, and a peaked one, which captures the cases of floods. This is nicely exemplified by displaying the monthly distribution of the water flow as provided in Figure 2: significant variations are apparent. Indeed, the streamflow of the river is more powerful in winter than in summer, and this is in line with the standard precipitation cycle in Italy, which exhibits a periodicity associated to the seasons. However, the highest streamflow peaks are all concentrated in November, even if the median value of the streamflow in that month is smaller than in the other winter months. This observation suggests that the maximum intensity of precipitations in the area is historically located in

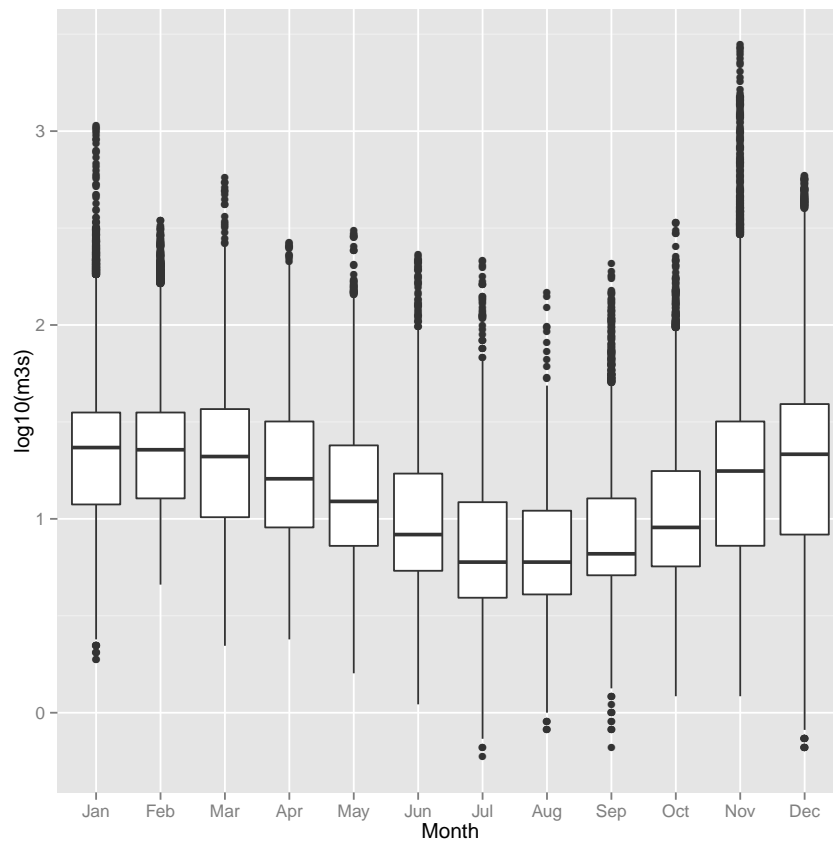


Figure 2: Distribution of the streamflow ( $\log_{10}(m^3/s)$ ) of the Paglia river by month.

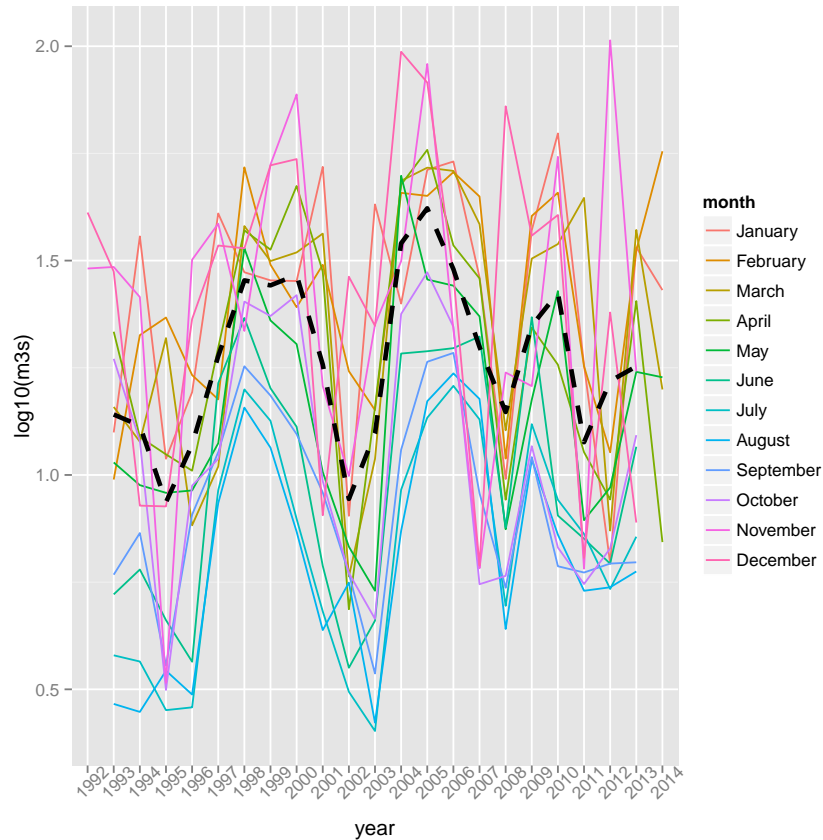


Figure 3: Evolution of monthly average streamflow ( $m^3/s$ ) of the Paglia river. The black dashed line represents the yearly average.

November, despite this month not being the most rainy one.

The evolution of the monthly averages is plotted in Figure 3. If the median streamflow is considered instead of the average, the overall picture remains substantially unchanged and is possibly even clearer (Figure 4). A cyclical pattern is apparent from the data, with a cycle whose period is about 5–7 years. This result suggests the existence of a relationship between rivers streamflow fluctuations and the periodicity of the oscillations of El Niño, which is recurrent on irregular intervals with an average period of 3–4 years; see, e.g., [[35, 36]]. However, it is worth to point out that the observed periodicities of these different phenomena do not perfectly match, indicating that further investigations are needed for a confirmation of this hypothesis. Furthermore, such a periodicity is also broadly in accordance with that of the North Atlantic Oscillations, whose fluctuations show a fairly regular periodic behavior over a time interval of 6–8 years [[4]].

Equally interesting is the evolution of the monthly maxima, reported in



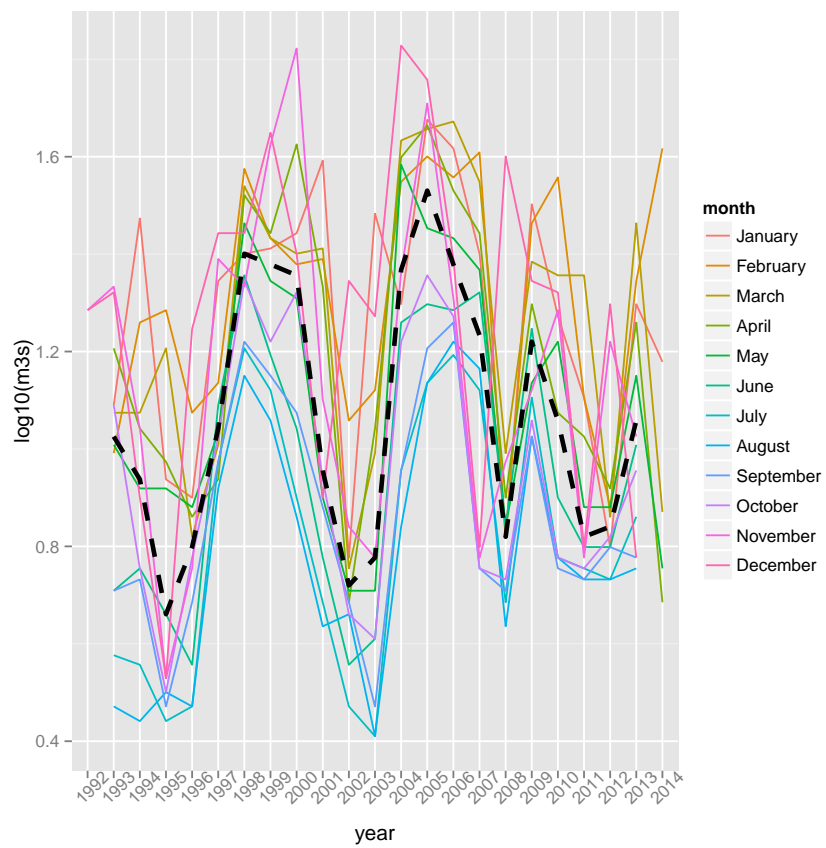


Figure 4: Evolution of monthly median streamflow ( $m^3/s$ ) of the Paglia river. The black dashed line represents the yearly median.

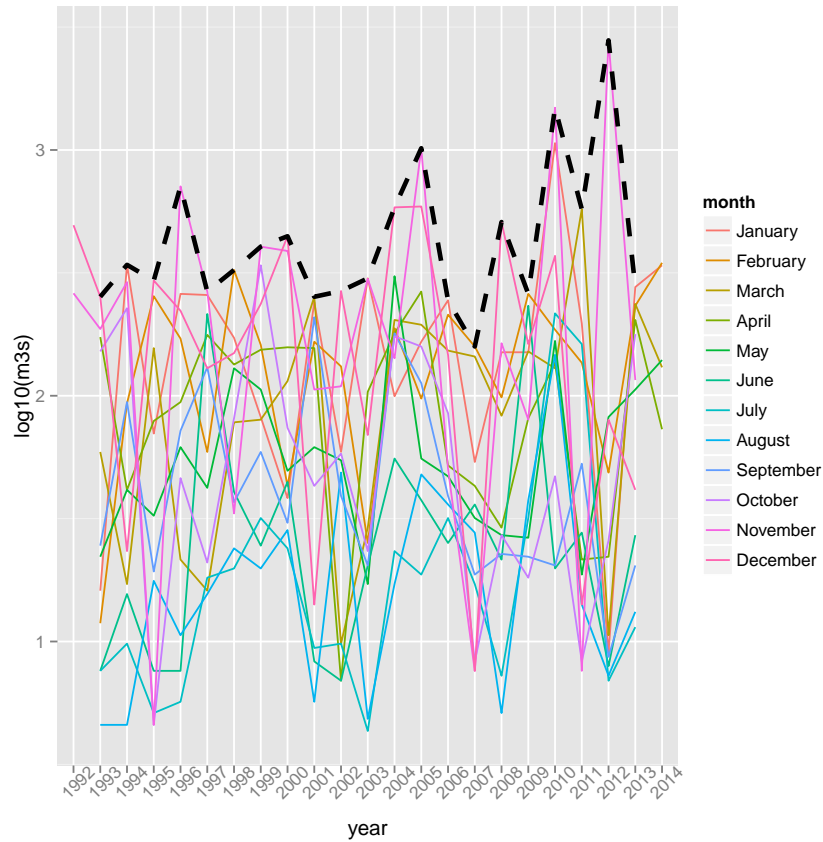


Figure 5: Evolution of monthly maxima ( $m^3/s$ ) of the Paglia river. The black dashed line represents the yearly maximum.

Figure 5, where a positive trend seems to exist in the recent annual maxima of the streamflow. This means that the intensity of the streamflow maxima has grown with respect to time in the last few years. This finding is in line with the overall climate change, which represents a severe and debated concern.

The rolling estimates of the Hurst exponent are plotted in Figure 6: at first sight this figure seems to suggest the presence of frequent large oscillations of the estimated values of the Hurst exponent in adjacent windows. In fact, this is not the case and this impression is mainly due to the high density of data points along the x-axis in the graph. A closer examination of the estimated values of the Hurst exponent reveals that there are few relatively large oscillations, related to an extreme event entering (or leaving) the estimation window. This effect is clearly visible in the fourth panel of Figure 6 that focuses on a subset of windows in the neighborhood of the negative spike depicted in the 400-day long windows panel. Here it can be

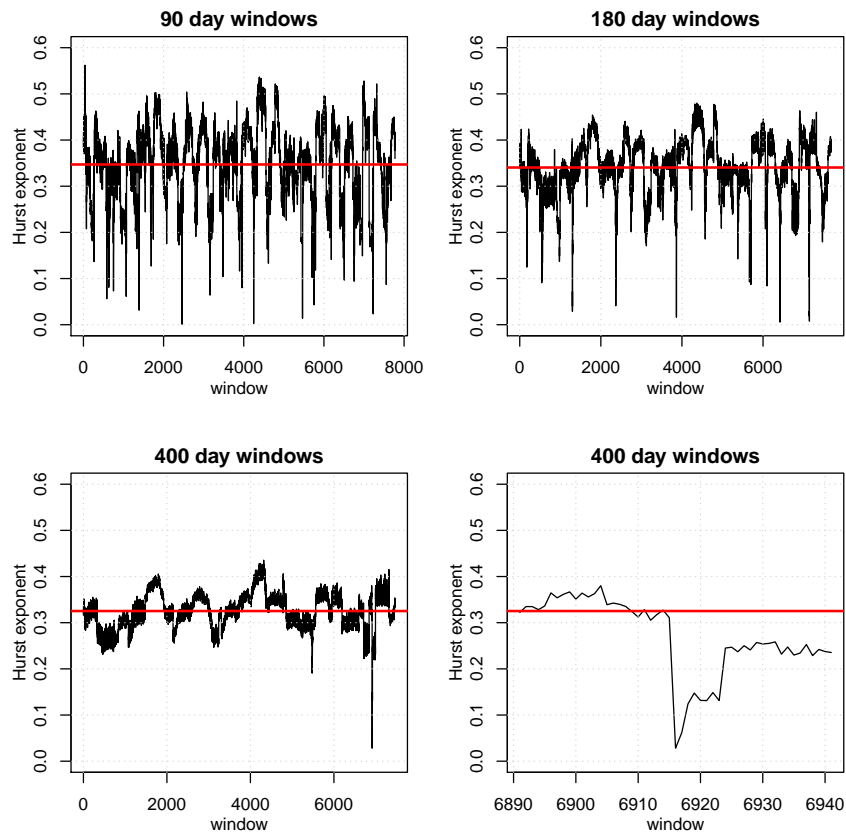


Figure 6: Estimated Hurst exponent over 90, 180, and 400-day long rolling windows. At each iteration the window is moved forward by a 1 day step. On the x-axis is reported chronological order given to windows. The horizontal red line is the average estimate of the Hurst exponent over all the windows. The fourth (lower-right) panel focuses on a subset of windows centred on the negative peak of the 400-day long windows estimates, corresponding to the first window containing November 12, 2012.

seen that the value of the Hurst exponent is fairly stable until the data of the flood of November 12, 2012 enter the estimation window: in coincidence with the new data entering the window, the estimated value of the Hurst exponent drops.

When considering 90-day long windows, 90% of the variations of the estimates across adjacent windows belong to the interval  $(-0.043, 0.046)$  and about 3.6% of them are larger than 0.05 in absolute value, whereas only 0.4% are larger than 0.1 (less than one third of the average value). Furthermore, 90% of the differences across adjacent 180-day long windows belong to the interval  $(-0.032, 0.034)$  and less than 0.1% of the variations are larger than 0.1 in absolute value: when 400-day windows are considered, these values become  $(-0.023, 0.022)$  and 0.03%, respectively (see Table 2). Note also that the estimated values are more stable for longer windows, as expected.

It is interesting also to observe that the average Hurst exponent over the rolling windows is about  $1/3$  (see again Table 2 and Figure 6). This value means that the series of the Paglia river streamflows is highly antipersistent. By analogy with financial econometrics based on DFA and time evolution of the Hurst exponent, this observation should lead to constructive risk assessment measures, but an application or discussion of this forecasting process falls outside the framework of the present paper. Uncertainty associated with the estimates is small, as can be observed from Table 2.

The estimates of the Hurst exponent seem to show a cyclical pattern, too. For this reason we carry out a spectral analysis of the series of the estimated Hurst exponents (see Figure 7) using an adaptive, sine multitaper power spectral density estimation method [[31]].

We are not now in the position to offer a definitive answer to this phenomenon. The apparent periodicity of the estimated Hurst exponent is probably influenced by the intrinsic features of the river streamflow: in particular, we observe that 2–3 days is the time interval required for the streamflow to return to the “normal” level preceding a peak, in the absence of further atmospheric phenomena. This is well illustrated in Figure 8, where the dynamics of the streamflow in the neighborhood of a number of peaks is compared: for ease of comparison, the peak heights are normalized to have the same range. We conjecture that the nonlinear, fairly recurrent, dynamics highlighted in Figure 8 may lay behind some of the observed periodicities of the Hurst exponent. This is not the only possible explanation, of course, and we acknowledge that the influence of several factors affecting the estimation of the Hurst exponent through DFA may be large and such to determine possible periodicities in the rolling estimates. To the best of our knowledge, a list of such factors should necessarily include the size of the time window, the number of data points in the window, the position of the windows on the

	90-day long windows		180-day long windows		400-day long windows	
	$H$	$\sigma_H$	$\Delta H$	$H$	$\sigma_H$	$\Delta H$
Min.	0.001	0.006	-0.230	0.006	0.008	-0.204
1st Q.	0.293	0.029	-0.015	0.308	0.035	-0.011
Median	0.357	0.040	0.000	0.343	0.041	0.000
Mean	0.347	0.040	0.000	0.340	0.042	0.000
3rd Q.	0.406	0.049	0.015	0.383	0.048	0.011
Max	0.562	0.201	0.195	0.480	0.204	0.148
$\sigma$	0.081	0.017	0.029	0.060	0.014	0.022
Skewness	-0.437	1.921	-0.355	-0.749	2.582	-0.659
Kurtosis	2.880	12.851	8.585	4.620	24.185	10.940
90% low	0.205	0.015	-0.043	0.253	0.023	-0.032
90% up	0.475	0.060	0.046	0.444	0.058	0.034
$\% \Delta H  > 0.05$			3.551			1.093
$\% \Delta H  > 0.075$			0.849			0.208
$\% \Delta H  > 0.1$			0.386			0.091
				$H$	$\sigma_H$	$\Delta H$
				0.028	0.019	-0.283
				0.300	0.036	-0.008
				0.324	0.042	0.000
				0.325	0.042	0.000
				0.353	0.047	0.008
				0.436		0.114
				0.038	0.139	0.014
				-0.239	3.083	-0.973
				3.795	21.881	26.402
				0.258	0.029	-0.023
				0.384	0.053	0.022
						0.188
						0.054
						0.027

Table 2: Descriptive statistics of the estimates of the Hurst exponent ( $H$ ), of its standard error ( $\sigma_H$ ), and of its variations in adjacent windows ( $\Delta H$ ). “90% low” and “90% up” describe the smallest intervals including 90% of the estimates.  $\%|\Delta H| > x$  denotes the percentage of variations in adjacent windows larger than  $x$  in absolute value.

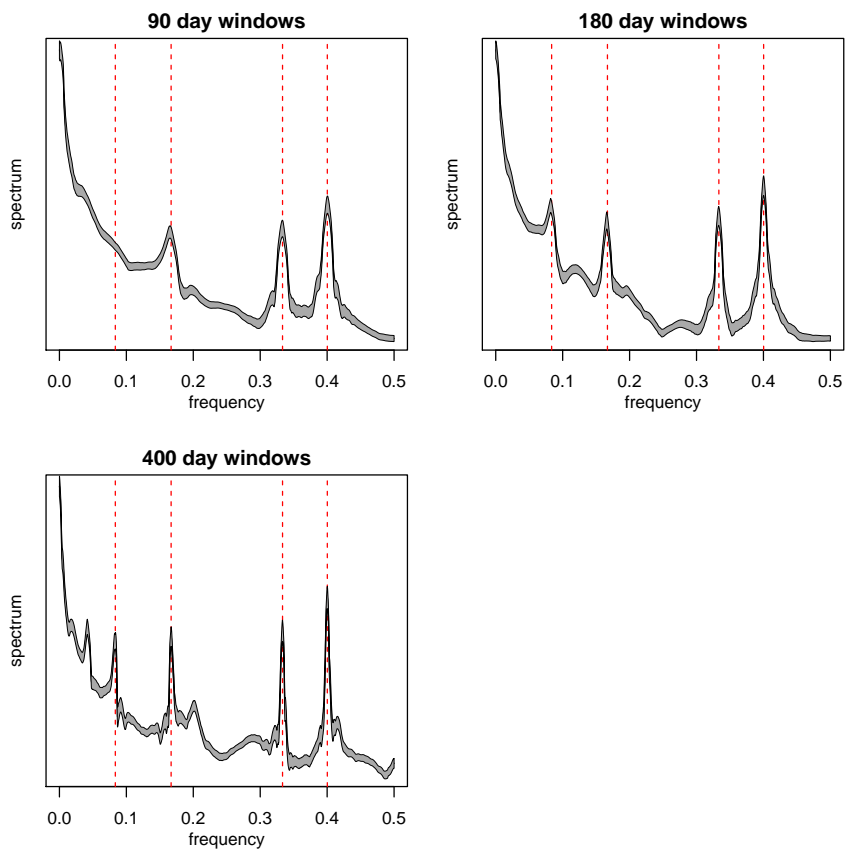


Figure 7: Estimated spectra of the series of the estimated Hurst exponents. The grey areas represent spectral uncertainties for 95% coverage probability. Peaks (from left to right) correspond to periodicities of about 12, 6, 3, and 2.5 days, respectively.

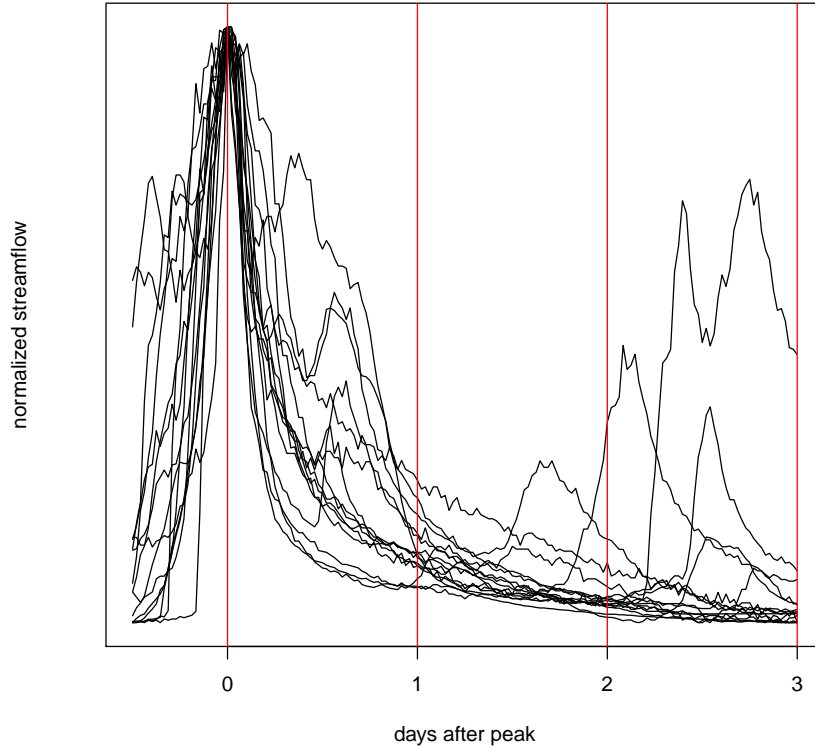


Figure 8: Comparison of the streamflow dynamics in the neighborhood of a number of peaks. The x-axis represent the distance from the peak expressed in days. The y-axis is the streamflow, normalized to have the same range across peaks.

time interval, the presence of heteroskedasticity in the original data. The literature lists important contributions dealing with estimation problems of the Hurst exponent and proposing methods beyond the DFA [[14, 37]] or with different tools like moving average techniques [[38, 39]]. Although this is beyond the scope of the present paper, the observed behavior of the spectrum of the Hurst exponent suggests to carry out further investigations on the estimation procedure of the Hurst exponent, possibly along the lines advocated in the contributions mentioned above. At any rate, the order of magnitude of the Hurst exponent given by the DFA is incontestable.

We want now to focus on a potential weakness in the data recording process. The validity check of the data, implemented through the consistency with Benford's law, leads us to observe a substantial failure: data seem to violate Benford's law (see Figure 9). Recall that Benford's law (BL) describes

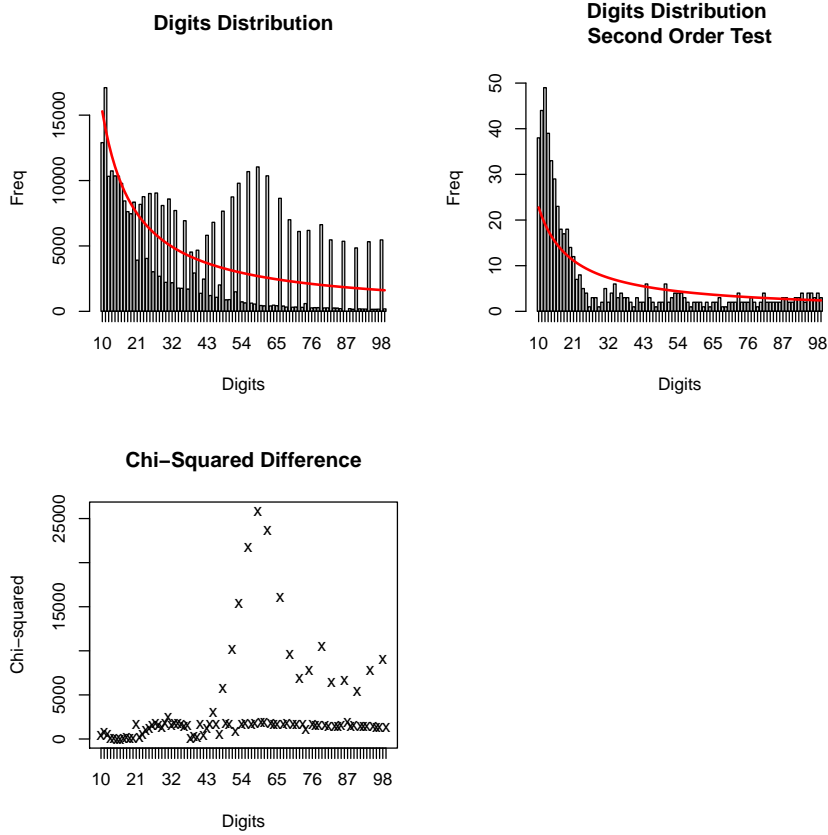


Figure 9: Benford's law first-two digits tests carried out on streamflow data ( $m^3/s$ ). Histograms represent the actual data distribution; the red solid curve is the theoretical Benford distribution.

the frequency distribution of leading digits in large data sets. In particular, Benford's law on the first digit (BL1) [[40, 16]] states that the distribution of the first digit is more concentrated on smaller values: the digit "1" has the highest frequency, "9" the lowest frequency. The first digit distribution follows a logarithmic law:

$$P(d) = \log_{10} \left( 1 + \frac{1}{d} \right), \quad d = 1, 2, \dots, 9, \quad (1)$$

where  $P(d)$  is the probability that the first digit is equal to  $d$  in the data set;  $\log_{10}$  being the logarithm in base 10.

There is a reasonable interpretation of the outcome of the inconsistency of the data with the regularity imposed by Benford's law. Flows ( $m^3/s$ ) are computed from water height, which is the really monitored quantity. However, water height is recorded with one centimeter precision, so that



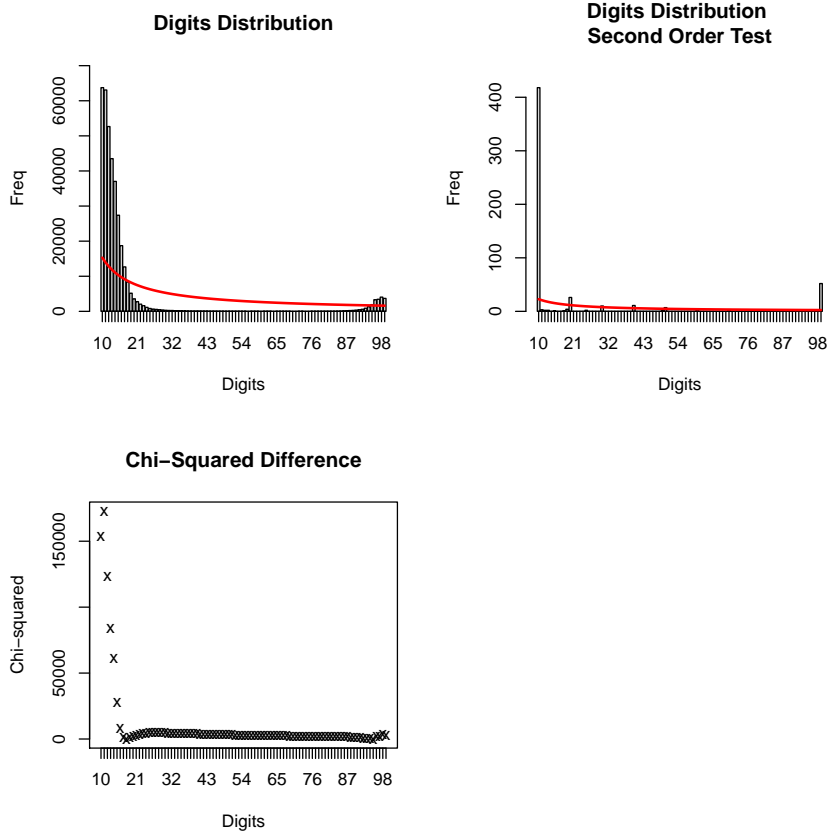


Figure 10: Benford's law first-two digits tests carried out on measured water heights (*cm*). Histograms represent the actual data distribution; the red solid curve is the theoretical Benford distribution.

many repeated values are possible. In fact, the two most common values are repeated more than 10,000 times (see Table 3). The analysis repeated on water heights (measured in centimeters) reveals that the distribution of water heights does not conform to Benford's law either (see Figure 10). In fact, this is practically annoying when looking for streamflow fluctuations in predictive analyses.

Finally, looking for other important data regularities, we argue that a plot of the (log-)size against the rank of the river's streamflow (see Figure 11) suggests that this relation can be well approximated by a discrete generalized Beta distribution (DGBD) of the form

$$f(r) = \frac{A(N + 1 - r)^b}{r^a} \quad (2)$$

where  $r$  is the rank,  $N := \max(r)$ , and  $A$ ,  $a$ , and  $b$  are parameters to be

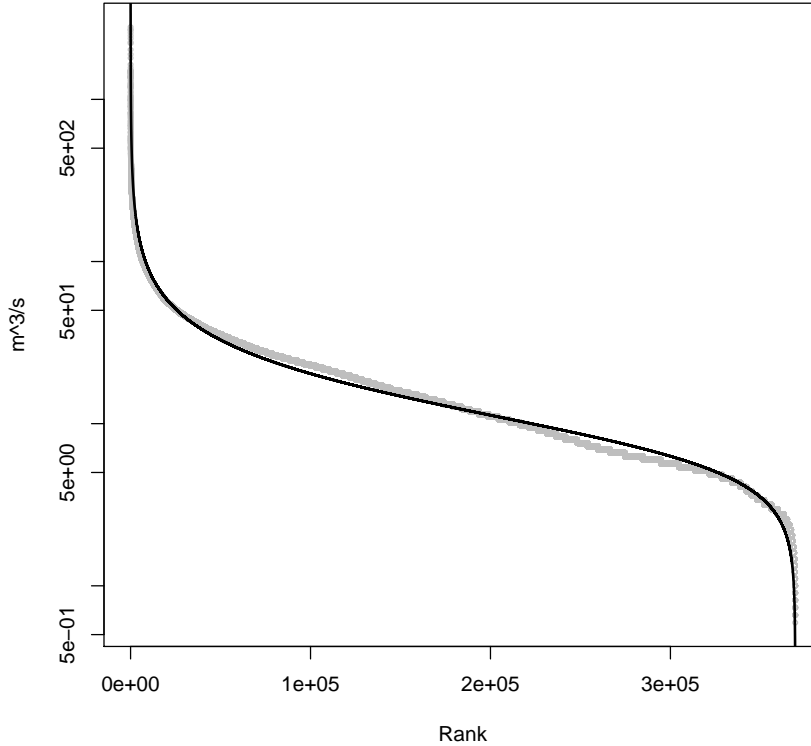


Figure 11: Rank-size relation of the Paglia river streamflow (data points are represented in grey). The continuous curve is the fit of a discrete generalized Beta distribution with  $(A, a, b, R^2) = (163.117, 0.596, 0.382, 0.986)$ .

estimated from the data.<sup>2</sup> This is indeed the case, and the  $R^2$  of the approximating function is  $R^2 \approx 0.986$ , confirming the “universality” of the DGBD suggested in other fields of investigation [[41, 42]], particularly in relation to complex phenomena characterized by the co-existence of many subsystems whose interactions produce the observed outcome [[34]].

## 4 Conclusions

This paper presents the analysis of the Paglia river streamflow. The dataset used is of large size: the considered series has 30-minutes period over a time-span of more than 22 years. The data series is antipersistent, with an average Hurst exponent of about  $1/3$ . This gives a precise information on how one

<sup>2</sup>Parameters can be estimated by Ordinary Least Squares from the model in logarithms.

$m^3/s$	freq
5.9833	10061
5.6859	10014
6.2890	9940
5.3968	9086
6.6030	8263
5.1161	7978
4.8436	6784
6.9253	6698
7.9420	6361
7.5948	5881

Table 3: Frequencies of the ten most common values.

can do forecast on the overflow of the considered river. Furthermore, we show that in recent years there has been an increasing trend in the maxima of the river streamflows, and a periodicity which broadly suggests a connection of the streamflows with El Niño and the North Atlantic Oscillations. However, more accurate measurements of the streamflow could be useful in having a more consistent dataset. We also show that the Paglia river streamflow is well represented by a discrete generalized beta distribution, congruent with the observed river discharge being the result of the interaction of many complex subsystems.

## Acknowledgements

We would like to thank three anonymous referees for their constructive comments that helped us to substantially improve the paper upon the previous versions. We are pleased to thank Guido Calenda and Elena Volpi for having provided us with the data. Funding from the Italian Ministry of Education, University and Research (PRIN grant code 201002AXKAJ\_005) is gratefully acknowledged.

## References

- [1] Hurst, H. E., (1951). Long-term storage capacity of reservoirs. Transactions of the American Society of Civil Engineers 116, 770-808.
- [2] Tessier, Y., Lovejoy, S., Hubert, P., Schertzer, D., Pecknold, S., (1996). Multifractal analysis and modeling of rainfall and river flows and scaling,

- causal transfer functions. *Journal of Geophysical Research: Atmospheres* 101 (D21), 26427-26440.
- [3] Pandey, G., Lovejoy, S., Schertzer, D., (1998). Multifractal analysis of daily river flows including extremes for basins of five to two million square kilometres, one day to 75 years. *Journal of Hydrology* 208 (1), 62-81.
  - [4] Collette, C., Ausloos, M., (2004). Scaling analysis and evolution equation of the North Atlantic oscillation index fluctuations. *International Journal of Modern Physics C* 15 (10), 1353-1366.
  - [5] Koscielny-Bunde, E., Kantelhardt, J. W., Braun, P., Bunde, A., Havlin, S., (2006). Long-term persistence and multifractality of river runoff records: Detrended fluctuation studies. *Journal of Hydrology* 322 (1), 120-137.
  - [6] Movahed, M. S., Hermanis, E., (2008). Fractal analysis of river flow fluctuations. *Physica A: Statistical Mechanics and its Applications* 387 (4), 915-932.
  - [7] Hajian, S., Movahed, M. S., (2010). Multifractal detrended cross-correlation analysis of sunspot numbers and river flow fluctuations. *Physica A: Statistical Mechanics and its Applications* 389 (21), 4942-4957.
  - [8] Peng, C.-K., Buldyrev, S. V., Havlin, S., Simons, M., Stanley, H. E., Goldberger, A. L., (1994). Mosaic organization of DNA nucleotides. *Physical Review E* 49 (2), 1685.
  - [9] Shlesinger, M., West, B., Klafter, J., (1987). Levy dynamics of enhanced diffusion: Application to turbulence. *Physical Review Letters* 58 (11), 1100.
  - [10] Ben-Avraham, D., Havlin, S., (2000). *Diffusion and reactions in fractals and disordered systems*. Cambridge University Press.
  - [11] Ivanova, K., Ausloos, M., (1999). Application of the detrended fluctuation analysis (DFA) method for describing cloud breaking. *Physica A: Statistical Mechanics and its Applications* 274 (12), 349-354.
  - [12] Ivanova, K., Clothiaux, E., Shirer, H., Ackerman, T., Liljegren, J., Ausloos, M., (2002). Evaluating the quality of ground-based microwave radiometer measurements and retrievals using detrended fluctuation and spectral analysis methods. *Journal of Applied Meteorology* 41 (1), 56-68.

- [13] Goldstein, M. L., Morris, S. A., Yen, G. G., (2004). Problems with fitting to the power-law distribution. *The European Physical Journal B-Condensed Matter and Complex Systems* 41 (2), 255-258.
- [14] Hu, K., Ivanov, P. C., Chen, Z., Carpena, P., Stanley, H. E., (2001). Effect of trends on detrended fluctuation analysis. *Physical Review E* 64 (1), 011114.
- [15] Nigrini, M. J., Miller, S. J., (2007). Benford's law applied to hydrology data - Results and relevance to other geophysical data. *Mathematical Geology* 39 (5), 469-490.
- [16] Benford, F., (1938). The law of anomalous numbers. *Proceedings of the American Philosophical Society* 78 (4), 551-572.
- [17] Judge, G., Schechter, L.,(2009). Detecting problems in survey data using Benford's law. *Journal of Human Resources* 44 (1), 1-24.
- [18] Clippe, P., Ausloos, M., (2012). Benford's law and Theil transform of financial data. *Physica A: Statistical Mechanics and its Applications* 391 (24), 6556-6567.
- [19] Mir, T., (2012). The law of the leading digits and the world religions. *Physica A: Statistical Mechanics and its Applications* 391 (3), 792-798.
- [20] Alves, A. D., Yanasse, H. H., Soma, N. Y., (2014). Benford's law and articles of scientific journals: Comparison of JCR R and Scopus data. *Scientometrics* 98 (1), 173-184.
- [21] Mir, T. A., Ausloos, M., Cerqueti, R., (2014). Benford's law predicted digit distribution of aggregated income taxes: the surprising conformity of Italian cities and regions. *The European Physical Journal B* 87 (11), 1-8.
- [22] Ausloos, M., Herteliu, C., Ileanu, B., (2015). Breakdown of Benford's law for birth data. *Physica A: Statistical Mechanics and its Applications* 419, 736-745.
- [23] Bormashenko, E., Shulzinger, E., Whyman, G., Bormashenko, Y., (2016). Benford's law, its applicability and breakdown in the IR spectra of polymers. *Physica A: Statistical Mechanics and its Applications* 444, 524-529.

- [24] Ausloos, M., Castellano, R., Cerqueti, R., (2016). Regularities and discrepancies of credit default swaps: a data science approach through Benford's law. *Chaos, Solitons & Fractals* 90, 8-17.
- [25] R Development Core Team, (2016). *R: A Language and Environment for Statistical Computing*. R Foundation for Statistical Computing, Vienna, Austria.  
URL <http://R-project.org>
- [26] Cinelli, C., (2016). *Benford.analysis: Benford Analysis for Data Validation and Forensic Analytics*. R package version 0.1.3.9000.  
URL <http://github.com/carloscinelli/benford.analysis>
- [27] Constantine, W., Percival, D., (2014). *fractal: Fractal Time Series Modeling and Analysis*. R package version 2.0-0.  
URL <https://CRAN.R-project.org/package=fractal>
- [28] Wickham, H.,(2009). *ggplot2: Elegant Graphics for Data Analysis*. Springer-Verlag, New York
- [29] Moritz, S., (2015). *imputeTS: Time Series Missing Value Imputation*. R package version 0.4.  
URL <https://CRAN.R-project.org/package=imputeTS>
- [30] Komsta, L., Novomestky, F., (2015). *moments: Moments, cumulants, skewness, kurtosis and related tests*. R package version 0.14.  
URL <https://CRAN.R-project.org/package=moments>
- [31] Barbour, A. J., Parker, R. L., (2014). *psd: Adaptive, sine multitaper power spectral density estimation for R*. *Computers & Geosciences* 63, 1-8.
- [32] Ryan, J. A., Ulrich, J. M., (2014). *xts: eXtensible Time Series*. R package version 0.9-7.  
URL <https://CRAN.R-project.org/package=xts>
- [33] Nigrini, M., (2012). *Benford's Law: Applications for Forensic Accounting, Auditing, and Fraud Detection*. John Wiley & Sons, Hoboken, NJ.
- [34] Naumis, G. G., Cocho, G., (2008). Tail universalities in rank distributions as an algebraic problem: The beta-like function. *Physica A: Statistical Mechanics and its Applications* 387 (1), 84-96.

- [35] Cane, M. A., Zebiak, S., Dolan, S., (1986). Experimental forecasts of El Nino. *Nature* 321, 827-832.
- [36] Eltahir, E. A., (1996). El Nino and the natural variability in the flow of the Nile river. *Water Resources Research* 32 (1), 131-137.
- [37] Chen, Z., Ivanov, P. C., Hu, K., Stanley, H. E., (2002). Effect of nonstationarities on detrended fluctuation analysis. *Physical Review E* 65 (4), 041107.
- [38] Vandewalle, N., Ausloos, M., (1998). Crossing of two mobile averages: A method for measuring the roughness exponent. *Physical Review E* 58 (5), 6832.
- [39] Vandewalle, N., Ausloos, M., Boveroux, P., (1999). The moving averages demystified. *Physica A: Statistical Mechanics and its Applications* 269 (1), 170-176.
- [40] Newcomb, S., (1881). Note on the frequency of use of the different digits in natural numbers. *American Journal of Mathematics* 4 (1), 39-40.
- [41] Martinez-Mekler, G., Martinez, R. A., del Rio, M. B., Mansilla, R., Miramontes, P., Cocho, G., (2009). Universality of rank-ordering distributions in the arts and sciences. *PLoS ONE* 4 (3), 1-7.
- [42] Ausloos, M., Cerqueti, R., (2016). A universal size-rank law, *PLoS ONE* (2016) 0166011.